N_2 Activation

DOI: 10.1002/anie.201005640

Unusually Strong Binding of Dinitrogen to a Ruthenium Center**

*Johanna M. Blacquiere, Carolyn S. Higman, Serge I. Gorelsky, Nicholas J. Beach, Scott J. Dalgarno, and Deryn E. Fogg**

Metal–dinitrogen complexes are of great interest for their potential to reduce energy costs in ammonia production, and to facilitate access to nitrogen-containing organic compounds.[1–3] Many examples have been discovered since the 1965 report[4] of $[Ru(NH_3)_5(N_2)]^{2+}$. Despite the prominence of iron systems in catalyzing the reduction of dinitrogen in industrial and biological contexts,[1,2a,3,5,6] and important recent advances in dinitrogen fixation by iron complexes,[1,7] early- and mid-transition metal complexes have shown greatest promise to date in cleaving the N–N bond.[1–3,8–11] A benchmark was set by Yandulov and Schrock, who reported molybdenum triamidoamine derivatives, the first well-defined catalysts capable of selectively reducing N_2 to ammonia.[12] Late-metal complexes tend to be limited by the lower energy of their d orbitals (which impedes back-donation into the high-energy N≡N antibonding orbitals),[13,14] and high N_2 lability. The latter has been identified as a key barrier to the development of late-metal catalysts for N_2 activation.[2a] Herein we present an experimental and computational study that addresses this barrier.

Our interest in the broad catalytic utility of hydridoruthenium complexes of N-heterocyclic carbene (NHC) ligands[15,16] led us to a report from Morris and co-workers describing synthesis of the activated IMes complex **2** (Scheme 1a; IMes = *N*,*N*′-bis(mesityl)imidazol-2-ylidene) through the thermolysis of **1** with excess IMes under argon.[17] We observed a very different reaction chemistry under an atmosphere of dinitrogen: $^{31}P\{^1H\}$ NMR analysis indicated the formation of less than 10% of **2** (59.35, 58.72 ppm; ABq, $^2J_{PP} = 13$ Hz, THF), but considerable free PPh_3 (Scheme 1b). The absence of any phosphine ligands in the major product **3** is evident from its null $^{31}P\{^1H\}$ NMR spectrum, and from the singlet multiplicity of its hydride signal. This species could be obtained free of **2** by carrying out the reaction at room temperature, and was isolated as an orange powder in 75% yield by precipitation from hexanes.

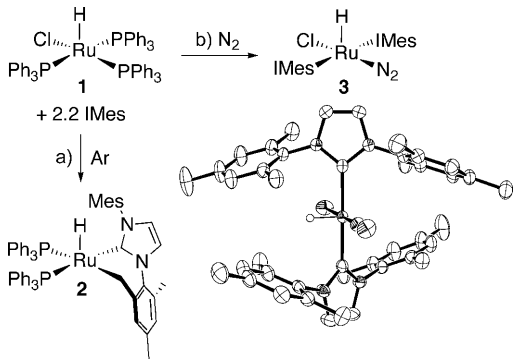

Scheme 1. Reaction of **1** with IMes under (a) Ar (12 h, THF, reflux); (b) N_2 (20 h, reflux or RT). The ORTEP diagram for **3**[35] shows non-hydrogen atoms as Gaussian ellipsoids set at the 50% probability level.

Single-crystal X-ray analysis of **3** indicated a mononuclear structure containing two mutually *trans*, unactivated IMes ligands (cf. the activated IMes group present in **2**). While disorder impeded the initial assignment of the remaining ligands, we identified **3** as $[RuHCl(IMes)_2(N_2)]$ by detailed NMR, IR, and MALDI-TOF mass spectrometric analysis. Refinement of the X-ray data with an appropriate disorder model yields a satisfactory solution. For both complexes in the unit cell, the N_2 and Cl sites are disordered over two positions (as found for other structures containing Cl *trans* to N_2);[18] in one, the hydride is also disordered over two positions. The excellent agreement between the model and the observed data provides unambiguous confirmation of connectivity, although the presence of the disorder limits the discussion of the metrical parameters.

The upfield location of the ^1H NMR singlet for the hydride ligand in **3** (−28.03 ppm; C_6D_6) is clear evidence for a square pyramidal complex with apical hydride. Integration confirms the presence of two IMes ligands. Rotation of $Ru-C_{NHC}$ and N–Mes bonds is rapid on the NMR timescale at 22 °C, as deduced from the equivalence of the mesityl *ortho*-CH_3 groups (these resolve into four singlets at 0 °C). The retention of chloride is confirmed by charge-transfer MALDI-TOF mass spectrometry,[19] which shows an excellent match between the simulated and observed isotope patterns for both $[RuHCl(IMes)_2(N_2)+H]^+$ (minor signal) and $[RuCl(IMes)_2-H]^{\cdot+}$ (major signal).[20] We initially ruled out the possibility that an N_2 ligand occupied the fifth coordination site on the basis of reactions with CO described below, but revised this conclusion in light of the quantitative formation

[*] J. M. Blacquiere, C. S. Higman, Dr. S. I. Gorelsky, N. J. Beach, Prof. D. E. Fogg
Department of Chemistry, and Centre for Catalysis Research & Innovation, University of Ottawa
Ottawa, K1N 6N5 (Canada)
E-mail: dfogg@uottawa.ca
Homepage: http://www.science.uottawa.ca/~dfogg/default.htm
Dr. S. J. Dalgarno
School of Engineering and Physical Sciences
Department of Chemistry, Heriot-Watt University
Edinburgh, EH14 4AS (UK)

[**] Supported by the Natural Sciences and Engineering Research Council (NSERC) of Canada. Ureshini Dharmasena is thanked for preliminary experimental work.

Supporting information for this article is available on the WWW under http://dx.doi.org/10.1002/anie.201005640.

of **3** on exposing $[RuHCl(IMes)_2(H_2)]$ to N_2. A natural-abundance ^1H–^{15}N NMR HSQC correlation experiment confirmed the coupling of hydride to a non-IMes ^{15}N nucleus (N_α: −72.6 ppm). The synthesis of $[^{15}N_2]$-**3** by reaction of **1** under 98% $^{15}N_2$ enabled the location of the $^{15}N\{^1H\}$ NMR signal for N_β as well (−55.8 ppm, d, $^1J_{NN} = 5$ Hz). The inequivalence of N_α and N_β supports identification of **3** as a monoruthenium, five-coordinate complex containing an end-bound, η^1-N_2 ligand, in which any end-over-end N_2 tumbling in solution is slow on the NMR timescale.

The IR spectrum of **3** revealed a single strong band at 2041 cm^{-1}, in the region expected for the ν(M-H) and ν(N≡N) vibrations. Isotopic-labeling experiments resulted in the expected shift in the ν(N≡N) band, to 1972 cm^{-1} for $[^{15}N_2]$-**3**: the ν(Ru-H) band appears essentially unperturbed, at 2039 cm^{-1}. Attempts to confirm the latter assignment by deuterium labeling were unsuccessful,[20] but the DFT-calculated ν(Ru-H) and ν(N≡N) values are very close, at 2187 and 2174 cm^{-1}, respectively.[21] The experimentally observed location of the ν(N≡N) band for **3**, at 2041 cm^{-1}, is striking in comparison to values for closely related phosphane derivatives, $[\{RuCl_2(Cy_2P(CH_2)_4PCy_2)_2\}(N_2)]$,[22] $[RuHCl(PCy_3)_2(N_2)]$,[23] and $[RuHCl(IMes)(PCy_3)(N_2)]$[16] (2124, 2060, and 2048 cm^{-1}, respectively). As the lowest energy of such band yet reported for a monometallic ruthenium complex,[24] this suggests considerable weakening of the N≡N bond.

Reactivity studies and computational analysis indicate an unexpectedly strong M–N_2 interaction in **3**. Remarkably, given the ease with which N_2 is normally lost in late-metal complexes (including closely related hydridoruthenium–NHC derivatives),[25–28] the N_2 ligand resists displacement by CO at room temperature. While exposure of **3** to CO effects immediate transformation, as indicated by a time-of-mixing color change of the solution from orange to pale yellow and an approximately 25 ppm downfield shift in the hydride singlet, the product is neither $[RuHCl(CO)(IMes)_2]$, nor dicarbonyl complex **5**[28] (Scheme 2). While **5** is indeed obtained under more forcing conditions (65% conversion in 1.5 hours at 65 °C; C_6D_6), the major product at 22 °C is the

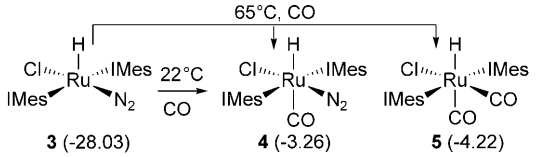

Scheme 2. Products formed upon reaction of **3** with CO. ^1H NMR chemical shifts for the hydride singlet (C_6D_6) shown in brackets.

mono-CO adduct **4** (90% yield; traces of **5** are also present). Formation of **4** reflects both the low lability of the N_2 ligand in **3**, which impedes access to the expected four-coordinate intermediate,[29] and the small size of the CO ligand.

In comparison, carbonylation of $[RuHCl(PCy_3)_2(N_2)]$ is much more facile, and yields 50% $[RuHCl(CO)_2(PCy_3)_2]$ within 20 minutes at room temperature.[23] The more forcing conditions required to convert **4** into **5** suggest that a strong Ru–N_2 interaction is retained in the former (although the presence of the π-acid CO ligand will undoubtedly attenuate N_2 binding relative to **3**). Unequivocal support for the assignment of **4** comes from the observation of a hydride singlet (−3.26 ppm; cf. −4.22 ppm for **5**) that exhibits a ^1H–^{13}C HMBC correlation with the equivalent carbene carbon nuclei and a new *C*O carbon nucleus (187.7 and 195.0 ppm, respectively): the large $^2J_{CH}$ value for the latter (49 Hz) is consistent with coupling to *trans* hydride. IR bands for ν(N≡N), ν(Ru-H), and ν(CO) appear at 2118, 2039, and 2005 cm^{-1}, respectively. Satisfactory microanalysis was hampered, however, by ligand loss under vacuum, and the presence of **5** in trace amounts.

Computational assessment of ligand-dissociation energies and the charge distribution in **3** was undertaken by analysis of the nontruncated system at the B3LYP[30]/DZVP[31] level of theory. Of note is the high dissociation energy calculated for the Ru–N_2 interaction (Table 1, entry 1), which exceeds the value calculated for the loss of IMes (17.8 vs. 14.6 kcal mol^{-1}),

Table 1: N_2 lability vs. N≡N activation in **3** and related complexes.[a]

Entry	Compound	ΔG_{298} [kcal mol^{-1}]	ν(N≡N) [cm^{-1}][21]	Atomic Charge [a.u.] N_α	N_β
1	$[RuHCl(IMes)_2(N_2)]$, **3**	17.8[b]	2174 [2041]	−0.02	−0.10
2	$[RuH_2(IMes)_2(N_2)]$, **3′**	5.2	2194	−0.06	−0.09
3	$[RuCl_2(IMes)_2(N_2)]$, **3″**	1.9	2235	−0.01	−0.05
4	$[Ru(NH_3)_5(N_2)](PF_6)_2$	13.6	2319 [2167][4]	−0.08	+0.13
5	$[FeH(depe)_2(N_2)](BPh_4)$[13]	n.g.	– [2091]	−0.09	+0.11
6	$[RuHCl(H_2IMes)_2(N_2)]$	17.2	2186	+0.04	−0.08
7	$[RuHCl(N_2)(PMe_3)_2]$	20.1	2216 [2060][c]	+0.02	−0.04
8	$[Mo(NN'_3)(N_2)]$[d, 13]	n.g.	– [1990][12b]	−0.07	−0.06

[a] Lability assessed from ΔG for N_2 loss; activation from both ν(N≡N) values (indicated as calculated [experimental] values), and atomic charges on N (assessed by natural-population analysis). [b] ΔG for loss of IMes = 14.6 kcal mol^{-1}. [c] Experimental value refers to the PCy_3 analogue. [d] N′ = 3,5-(2,4,6-*i*$Pr_3C_6H_2$)$_2C_6H_3$. Cy = cyclohexyl, depe = 1,2-bis(diethylphosphanyl)ethane.

despite the strength that is routinely attributed to M–NHC bonds.[32] Consistent with this finding is our unanticipated observation, in preliminary studies, that olefin isomerization via **3** is suppressed by added IMes: that is, the mechanism is dissociative in NHC.

We attribute the strong binding of the N_2 ligand in **3** to the simultaneous presence of a strongly σ-donating hydride ligand, and a π-donating chloride *trans* to N_2, as well as the donor properties of the two NHC ligands. A fragment molecular orbital (FMO) analysis of **3**, relative to complexes $[RuXX'(IMes)_2(N_2)]$ (**3′**: X = X′ = H; **3″**: X = X′ = Cl), gives more detailed insight. The energies of the d orbitals for the $[RuXX'(IMes)_2]$ fragment F1 increase in the order **3″** < **3** < **3′** (Figure 1a), reflecting the electrostatic repulsion associated with successive replacement of chloride by the strong σ-donor hydride. The high d-orbital energy of dihydride **3′** favors the F1→N_2 back-donation, owing to the improved match in

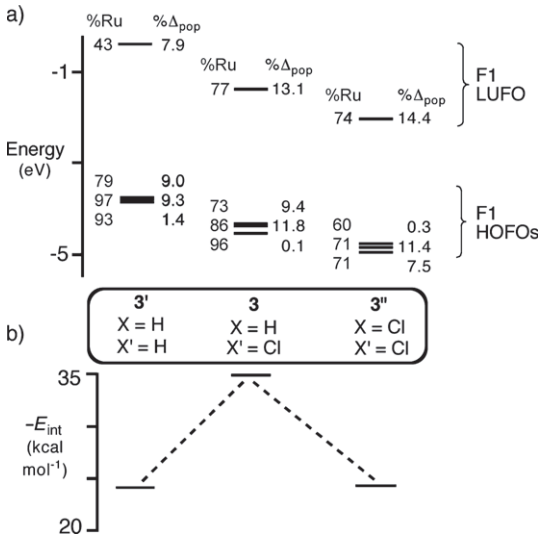

Figure 1. (a) Energies of frontier molecular orbitals of [RuXX′(IMes)$_2$], fragment (F1). %Ru = Ru character in fragment orbitals; $\%\Delta_{pop}$ = change in population on turning on the F1–N_2 interaction. (b) F1–N_2 electronic interaction energy ($-E_{int}$).

orbital energies, but limits σ donation from $N_2 \rightarrow$F1, as indicated by the lower electronic-interaction energy ($-E_{int}$; Figure 1b). Dramatically weaker N_2 binding results (Table 1, entry 2). In **3″**, conversely, σ donation is improved, but the low HOFO energies, and their reduced Ru character, limit effective π back-bonding. Again, this results in weakened $-E_{int}$ and Ru–N_2 bonding (Figure 1b; Table 1, entry 3). Complex **3** thus occupies a "sweet spot" maximizing both σ donation from $N_2 \rightarrow$F1, and back-donation from F1 into the N_2 antibonding orbital. The resulting stabilization presumably contributes to the activation barrier evident from the low N_2 lability for **3**. As regards N_2 activation, Tuczek and Lehnert[14] have pointed out the importance of strong σ-donor ligands: the present system illustrates the operation and limits of this effect, and the capacity of a π-donor ligand to significantly amplify it. It should be noted that the σ-donor ligand must be perpendicular to the M–N bond, so that its strong *trans* influence does not diminish the M–N_2 bond strength: this feature is "built in" to square pyramidal **3**, as the high *trans* influence of hydride constrains it to occupancy of the apical site.

The IMes ligand is unlikely to be unique in its capacity to simultaneously stabilize N_2 binding, and to activate the N_2 ligand, in this [RuHClL$_2$(N_2)] complex. To examine whether other strong σ-donor L-ligands exert a similar effect, we calculated the ΔG for N_2 loss, $\nu(N_2)$, and the atomic charge on N_2 for L = IMes, H_2IMes, and PMe_3 (Table 1). The strength of N_2 binding is comparably high for all three complexes, differing by only 2-3 kcal mol^{-1} (i.e. within error limits),[33] as compared to the 15 kcal mol^{-1} range for **3**–**3″**. N_2 activation, however, declines in the order L = IMes > H_2IMes > PMe_3. This difference reflects the greater role of σ donation in N_2 binding, but of π back-bonding in contributing to N≡N *activation*.

The electron density on the N_2 ligand in **3** suggests that it should be susceptible to electrophilic attack. Both N_α and N_β are negatively charged in all of complexes **3**–**3″** (Table 1, entries 1–3), in contrast to the Senoff complex (Table 1, entry 4), and Tuczek's iron complex (Table 1, entry 5). Indeed, the electron density on N_β in **3** exceeds that calculated for the Schrock Mo system (Table 1, entry 6), suggesting that this site should likewise react with Brønsted or Lewis acids. However, preliminary experiments with lutidinium BAr^F (with or without the reducing agent Cp_2Co),[12a] 9-BBN,[34] or NaH[7d] showed no change by ^{1}H or ^{1}H–^{15}N HSQC NMR analysis. This is almost certainly due to the steric protection of N_β conferred by the bulky IMes ligands, exacerbated by their rapid rotation at room temperature (see above); less encumbered systems are currently under study.

The foregoing describes a ruthenium–NHC complex that binds N_2 with unprecedented strength, thus demonstrating that the problem of high N_2 lability is not intrinsic to late-metal complexes, as heretofore believed. The heightened N_2 binding and activation found for [RuHCl(IMes)$_2$(N_2)], relative to its dihydride and dichloride analogues, in conjunction with the DFT-predicted stabilization of bound N_2 for analogous complexes containing other strong σ-donor L-ligands, suggest promising new directions for the design of robust late-transition-metal catalysts for dinitrogen functionalization.

Experimental Section

Optimized synthesis of **3**:[20] Solid IMes (359 mg, 1.812 mmol, 2.2 equiv), followed by THF (5 mL), was added to a stirred suspension of **1** (496 mg, 0.537 mmol) in THF (9 mL) under N_2. A color change from purple to orange was evident over 20 h at 24 °C. ^{31}P NMR analysis at this point revealed only the presence of free PPh_3. The dark orange solution was filtered through Celite, the solvent was removed under reduced pressure and the residue was taken up in hexanes. The resulting suspension was chilled (−35 °C), filtered, and washed with cold hexanes (3 mL) and hexanes/Et_2O (3:1; 3 × 1 mL). The orange solid was dried under vacuum. Yield 309 mg (74 %). ^{1}H NMR (C_6D_6, 298 K): δ = 6.84 (s, Mes C*H*, 4H), 6.82 (s, Mes C*H*, 4H), 6.25 (s, NC*H*, 4H), 2.34 (s, Mes *p*-CH_3, 12H), 2.14–2.08 (br, Mes *o*-CH_3, 24H), −28.03 ppm (s, Ru*H*, 1H). At 203 K, the signal for the mesityl C*H* protons resolves into two singlets, and those for the methyl protons into six singlets. ^{13}C{^{1}H} NMR (C_6D_6, 298 K): δ = 198.4 (s, RuC_{NHC}), 150.3 (Mes *i*-*C*), 136.9 (Mes *p*-*C*), 129.1 (Mes *C*H), 128.4 (Mes *i*-*C*), 121.7 (s, N*C*H), 21.3 (s, Mes *p*-*C*H_3), 19.0 ppm (br s, Mes *o*-*C*H_3). ^{15}N{^{1}H} NMR (C_6D_6, 30 MHz): δ = −55.8 (d, $^1J_{NN}$ = 5 Hz, N_β), −72.6 ppm (d, $^1J_{NN}$ = 5 Hz, N_α). IR (Nujol): ν(Ru-H), $\nu(N_2)$ 2041 cm^{-1} ([$^{15}N_2$]-**3**: ν(Ru-H) 2039 cm^{-1}, ν(^{15}N≡^{15}N) 1972 cm^{-1}). CT-MALDI MS (pyrene matrix), *m*/*z*: [RuHCl(IMes)$_2$(N_2)+H]$^+$ 775.1 (simulated: 775.3); [RuCl(IMes)$_2$−H]$^+$ 744.3 (simulated: 744.3). Anal. Calcd. for $C_{42}H_{49}ClN_6Ru$: C, 65.14; H, 6.38; N, 10.85. Found: C, 65.22; H, 6.27; N, 10.78.

Synthesis of [RuHCl(CO)(IMes)$_2$(N_2)] **4**:[20] A solution of [RuHCl(IMes)$_2$(N_2)] (70 mg, 0.090 mmol) in C_6H_6 (2 mL) was degassed by consecutive freeze-pump-thaw cycles and allowed to thaw under 1 atm of CO at room temperature. A color change from orange to pale yellow was complete within 5 min. The solvent was removed under reduced pressure to obtain a pale yellow solid. Yield 66 mg (90 %). ^{1}H NMR (C_6D_6, 500 MHz): δ = 6.77 (s, Mes C*H*, 4H), 6.75 (s, Mes C*H*, 4H), 6.13 (s, NC*H*, 4H), 2.24 (s, Mes *p*-CH_3, 12H), 2.15 (s, Mes *o*-CH_3, 12H), 2.13 (s, Mes *o*-CH_3, 12H), −3.26 ppm (s, Ru*H*, 1H). ^{13}C{^{1}H} NMR (C_6D_6, 298 K, 126 MHz): δ = 195.0 (s, *C*O), 187.7 (s, RuC_{NHC}), 139.4 (s, Mes *i*-*C*), 137.2 (s, Mes *p*-*C*), 136.7 (s, Mes *o*-*C*′), 136.4 (s, Mes *o*-*C*), 129.43 (s, Mes *C*H), 129.37 (s, Mes *C*H),

123.2 (s, NCH), 21.3 (s, Mes *p*-CH_3), 18.8 (s, Mes *o*-CH_3), 18.7 ppm (s, Mes *o*-CH_3). ^{13}C (^1H-coupled) NMR: $\delta = 195.0$ (d, $^2J_{CH} = 49$ Hz, *C*O), 187.7 (d, $^2J_{CH} = 5$ Hz, RuC_{NHC}). IR (Nujol): $\nu(N_2)$, 2118 cm^{-1}; ν(Ru-H), 2039 cm^{-1}; ν(CO), 2005 cm^{-1}. Microanalysis is consistently poor, owing to the presence of ca. 5% of **5**, and ligand loss upon extended exposure to reduced pressure to remove traces of the solvent.

Received: September 8, 2010
Revised: November 29, 2010
Published online: December 29, 2010

Keywords: carbene ligands · density functional calculations · dinitrogen activation · hydrides · ruthenium

[1] J. L. Crossland, D. R. Tyler, *Coord. Chem. Rev.* **2010**, *254*, 1883–1894.
[2] a) B. A. MacKay, M. D. Fryzuk, *Chem. Rev.* **2004**, *104*, 385–401; b) M. D. Fryzuk, *Acc. Chem. Res.* **2009**, *42*, 127–133; c) L. P. Spencer, B. A. MacKay, B. O. Patrick, M. D. Fryzuk, *Proc. Natl. Acad. Sci. USA* **2006**, *103*, 17094–17098.
[3] C. M. Kozak, P. Mountford, *Angew. Chem.* **2004**, *116*, 1206–1209; *Angew. Chem. Int. Ed.* **2004**, *43*, 1186–1189.
[4] A. D. Allen, C. W. Senoff, *Chem. Commun.* **1965**, 621–622.
[5] J. B. Howard, D. C. Rees, *Chem. Rev.* **1996**, *96*, 2965–2982.
[6] B. M. Barney, D. Lukoyanov, T.-C. Yang, D. R. Dean, B. M. Hoffman, L. C. Seefeldt, *Proc. Natl. Acad. Sci. USA* **2006**, *103*, 17113–17118.
[7] Selected recent examples: a) Y. Lee, N. P. Mankad, J. C. Peters, *Nat. Chem.* **2010**, *2*, 558–565; b) L. D. Field, H. L. Li, A. M. Magill, *Inorg. Chem.* **2009**, *48*, 5–7; c) J. J. Scepaniak, J. A. Young, R. P. Bontchev, J. M. Smith, *Angew. Chem.* **2009**, *121*, 3204–3206; *Angew. Chem. Int. Ed.* **2009**, *48*, 3158–3160; d) J. Scott, I. Vidyaratne, I. Korobkov, S. Gambarotta, P. H. M. Budzelaar, *Inorg. Chem.* **2008**, *47*, 896–911; e) J. M. Smith, A. R. Sadique, T. R. Cundari, K. R. Rodgers, G. Lukat-Rodgers, R. J. Lachicotte, C. J. Flaschenriem, J. Vela, P. L. Holland, *J. Am. Chem. Soc.* **2006**, *128*, 756–769; f) J. D. Gilbertson, N. K. Szymczak, D. R. Tyler, *J. Am. Chem. Soc.* **2005**, *127*, 10184–10185.
[8] D. J. Knobloch, E. Lobkovsky, P. J. Chirik, *Nat. Chem.* **2010**, *2*, 30–35.
[9] G. B. Nikiforov, I. Vidyaratne, S. Gambarotta, I. Korobkov, *Angew. Chem.* **2009**, *121*, 7551–7555; *Angew. Chem. Int. Ed.* **2009**, *48*, 7415–7419.
[10] J. Ballmann, R. F. Munha, M. D. Fryzuk, *Chem. Commun.* **2010**, *46*, 1013–1025.
[11] S. Gambarotta, J. Scott, *Angew. Chem.* **2004**, *116*, 5412–5422; *Angew. Chem. Int. Ed.* **2004**, *43*, 5298–5308.
[12] a) D. V. Yandulov, R. R. Schrock, *Science* **2003**, *301*, 76–78; b) D. V. Yandulov, R. R. Schrock, A. L. Rheingold, C. Ceccarelli, W. M. Davis, *Inorg. Chem.* **2003**, *42*, 796–813; c) D. V. Yandulov, R. R. Schrock, *J. Am. Chem. Soc.* **2002**, *124*, 6252–6253.
[13] F. Studt, F. Tuczek, *J. Comput. Chem.* **2006**, *27*, 1278–1291.
[14] F. Tuczek, N. Lehnert, *Angew. Chem.* **1998**, *110*, 2780–2782; *Angew. Chem. Int. Ed.* **1998**, *37*, 2636–2638.
[15] S. D. Drouin, G. P. A. Yap, D. E. Fogg, *Inorg. Chem.* **2000**, *39*, 5412–5414.
[16] N. J. Beach, J. M. Blacquiere, S. D. Drouin, D. E. Fogg, *Organometallics* **2009**, *28*, 441–447.
[17] K. Abdur-Rashid, T. Fedorkiw, A. J. Lough, R. H. Morris, *Organometallics* **2004**, *23*, 86–94.
[18] J. N. Coalter, J. C. Bollinger, J. C. Huffman, U. Werner-Zwanziger, K. G. Caulton, E. R. Davidson, H. Gerard, E. Clot, O. Eisenstein, *New J. Chem.* **2000**, *24*, 9–26.
[19] M. D. Eelman, J. M. Blacquiere, M. M. Moriarty, D. E. Fogg, *Angew. Chem.* **2008**, *120*, 309–312; *Angew. Chem. Int. Ed.* **2008**, *47*, 303–306.
[20] For details, including full spectra, see the Supporting Information.
[21] Trends in calculated IR frequencies (i.e. relative values) are significant, although absolute values should be treated with caution, given the limited precision of current DFT methods for vibrational analyses. See: W. Koch, M. C. Holthausen, *A Chemist's Guide to Density Functional Theory*, *2nd ed.*, Wiley, New York, **2001**.
[22] D. Amoroso, G. P. A. Yap, D. E. Fogg, *Can. J. Chem.* **2001**, *79*, 958–963.
[23] M. Oliván, K. G. Caulton, *Inorg. Chem.* **1999**, *38*, 566–570.
[24] A $\nu(N_2)$ value of 2019 cm^{-1} was found for a tetranuclear Ru/Ir cluster, see: H. Mori, H. Seino, M. Hidai, Y. Mizobe, *Angew. Chem.* **2007**, *119*, 5527–5530; *Angew. Chem. Int. Ed.* **2007**, *46*, 5431–5434.
[25] A. C. Bowman, C. Milsmann, C. C. Hojilla Atienza, E. Lobkovsky, K. Wieghardt, P. J. Chirik, *J. Am. Chem. Soc.* **2010**, *132*, 1676–1684.
[26] A. M. Archer, M. W. Bouwkamp, M.-P. Cortez, E. Lobkovsky, P. J. Chirik, *Organometallics* **2006**, *25*, 4269–4278.
[27] S. Burling, L. J. L. Haller, E. Mas-Marza, A. Moreno, S. A. MacGregor, M. F. Mahon, P. S. Pregosin, M. K. Whittlesey, *Chem. Eur. J.* **2009**, *15*, 10912–10923.
[28] J. P. Lee, Z. Ke, M. A. Ramirez, T. B. Gunnoe, T. R. Cundari, P. D. Boyle, J. L. Petersen, *Organometallics* **2009**, *28*, 1758–1775.
[29] Five-coordinate ruthenium complexes bearing bulky donor ligands commonly react through a dissociative pathway, and the energetic accessibility of four-coordinate "sawhorse" structures is very well established, see: D. Huang, W. E. Streib, J. C. Bollinger, K. G. Caulton, R. F. Winter, T. Scheiring, *J. Am. Chem. Soc.* **1999**, *121*, 8087–8097. A dynamic equilibrium is reported between [RuH(CO)$(IMes)_2(N_2)$] BAr^F and its N_2-free derivative: see Ref. [28].
[30] A. D. Becke, *J. Chem. Phys.* **1993**, *98*, 5648–5652.
[31] N. Godbout, D. R. Salahub, J. Andzelm, E. Wimmer, *Can. J. Chem.* **1992**, *70*, 560–571.
[32] F. E. Hahn, M. C. Jahnke, *Angew. Chem.* **2008**, *120*, 3166–3216; *Angew. Chem. Int. Ed.* **2008**, *47*, 3122–3172.
[33] The slower carbonylation of **3** vs. [RuHCl$(PCy_3)_2(N_2)$] implies that **3** binds N_2 more strongly. The discrepancy with the ΔG data could be a result of the uncertainties in the latter; limitations on PMe_3 as a model for PCy_3 (space-filling models support a steric role for PCy_3 in promoting N_2 loss); or greater weakening of the Ru–N_2 bond in the [RuHClL_2(CO)(N_2)] adduct where L = PCy_3, vs. IMes. Irrespective of the precise magnitude and order of ΔG, however, it is clear that other strong L-donors are likewise able to stabilize N_2 binding.
[34] M. D. Fryzuk, B. A. MacKay, S. A. Johnson, B. O. Patrick, *Angew. Chem.* **2002**, *114*, 3861–3864; *Angew. Chem. Int. Ed.* **2002**, *41*, 3709–3712.
[35] CCDC 792128 contains the supplementary crystallographic data for this paper. These data can be obtained free of charge from The Cambridge Crystallographic Data Centre via www.ccdc.cam.ac.uk/data_request/cif. Refined formula, $C_{42}H_{48.75}ClN_6Ru$; formula weight, 774.14; crystal dimensions, $0.08 \times 0.07 \times 0.05$ mm; crystal system, monoclinic; space group, *C*2/*c*; unit cell dimensions, $a = 20.985(4)$ Å, $\alpha = 90°$, $b = 20.967(3)$ Å, $\beta = 109.171(3)°$, $c = 19.412(3)$ Å, $\gamma = 90°$; 8068(2) $Å^3$; Z, 8; ρ_{calc}, 1.275 Mg/m^3; linear absorption coefficient, 0.491 mm^{-1}; wavelength, 0.71073 Å; temp., 173(2) K; collection range, $1.41 \le \theta \le 27.11°$; reflections collected, 28361; independent reflections, 8841 [R(int) = 0.0306]; observed reflections, 6548 [$I > 2\sigma(I)$]; final R indices [$I > 2\sigma(I)$], $R_1 = 0.0349$ and $wR_2 = 0.0956$; R indices (all data), $R_1 = 0.0518$, $wR_2 = 0.1048$.

